Available online at www.sciencedirect.com
ScienceDirect
Journal of Fluorine Chemistry 128 (2007) 285–295
JOURNAL OF FLUORINE CHEMISTRY
www.elsevier.com/locate/fluor

Review

Role of elemental fluorine in nuclear field

H. Groult [a,*], F. Lantelme [a], M. Salanne [a], C. Simon [a], C. Belhomme [b], B. Morel [b], F. Nicolas [c]

[a] *Université P. & M. Curie-Paris 6, CNRS-UPMC-ESPCI UMR 7612, Laboratoire LI2C, 4 Place Jussieu, Paris F-75005, France*
[b] *Areva NC, Laboratoire R&D, BP 29, 26700 Pierrelatte Cedex, France*
[c] *Cogema-Areva, Laboratoire R&D, BP 16, 26700 Pierrelatte Cedex, France*

Received 1 October 2006; received in revised form 13 November 2006; accepted 17 November 2006
Available online 28 November 2006

Dedicated to Professor Neil Bartlett on the occasion of this 75th birthday.

Abstract

The preparation of fluorine gas by Henri Moissan by electrolysis of molten fluorides can be considered as one of the most important discoveries during the last centuries. Indeed, in addition to its use in many industrial fields (microelectronic, surface cleaning, pharmacology, medicine, ...), fluorine gas is strongly involved in nuclear field for the preparation of UF_6. The latter allows the natural uranium enrichment *via* the gaseous diffusion process. Due to the increase of the energy demand in industrialised and emergent countries, the production of UF_6 and consequently of F_2 should increase drastically during the next decades. The aim of this paper is to summarise the evolution of the process to produce fluorine from its discovery to the present process. Few aspects on the researches done for a better understanding of the fluorine evolution reaction are presented. The use of fluorine in the nuclear field is also discussed.

Keywords: Henri Moissan; KF–2HF; Fluorine; UF_6; Isotopic enrichment

Contents

1. Introduction

Fluorine is derived from the Latin word ''*fluere*,'' meaning to flow. It never occurs as a free element in nature and is most commonly found in the minerals. Fluorides are well known

* Corresponding author. Tel.: +33 1 4427 3534; fax: +33 1 4427 3856.
E-mail address: groult@ccr.jussieu.fr (H. Groult).

0022-1139/$ – see front matter © 2006 Elsevier B.V. All rights reserved.
doi:10.1016/j.jfluchem.2006.11.012

since several centuries. For example, fluorite also called fluorspar (CaF_2) was described since 1530 by Georgius Agricola who reported how the addition of fluxes such as CaF_2, which acts as a solvent for ores, facilitates the smelting of ores. In other words, fluorspar allows to promote the fusion of metals or minerals. In 1670, Heinrich Schwanhard observed the attack of glass by fumes obtained by slowly heating in a glass retort of a mixture of fluorspar and sulphuric acid. One century later, the Swedish apothecary Carl Wilhelm Scheele studied in detail the chemical nature of fluorspar and the details of its reaction with acids. He was followed by numerous of brilliant scientists such as Humphry Davy, Gay-Lussac, Antoine Lavoisier and Louis Thénard who made different kinds of experiments with hydrofluoric acid obtained from the chemical reaction between fluorspar and sulphuric acid. At this time, it was admitted that hydrofluoric acid contained a new element having properties similar to chlorine. Then, many efforts have been done to isolate this unknown element but it was revealed to be a very difficult challenge due to the extreme reactivity of fluorine. It was finally achieved in 1886 when Ferdinand-Frédéric-Henri Moissan (Fig. 1) succeeded in insulating fluorine.

Owing to this discovery, Henri Moissan won the 1906 Nobel Prize in Chemistry. Henri Moissan performed the electrolysis of a solution of potassium hydrogen fluoride (KHF_2) in liquid hydrogen fluoride (HF). Still today, elemental fluorine is industrially prepared using the Moissan's process. Nowadays, fluorine gas can be produced with a very high purity level and find many applications in various industrial fields: for the preparation of SF_6 (gaseous electrical insulator), NF_3 (etching agent in microelectronic), WF_6 (CVD deposition), ClF_3 (microelectronic, etching of diffusion barrier, ...), mixture of F_2 and N_2 (impermeabilisation of gasoline tanks). Fluorine gives chlorofluorocarbons such as dichlorodifluoromethane (CF_2Cl_2) which was widely used in air conditioning and cooling systems and in aerosol spray cans. Nevertheless, efforts have been done to remove these compounds because they were causing damages to the Earth's ozone layer. The reaction of fluorine and carbon also gives rise to the formation of solid fluorocarbon compounds which have been commercially used since the 1970s in primary lithium batteries. One of the main uses of fluorine is related to the manufacture of uranium hexafluoride UF_6 which allows the isotopic enrichment of natural uranium. About 60% of the world production of F_2 is devoted to the synthesis of this gaseous fluoride compound. For this reason, elemental fluorine can be considered as a key element for the preparation of electricity *via* nuclear plants. This point will be discussed hereafter.

Fig. 1. Henri Moissan (1852–1907) who won the 1906 Nobel Prize in Chemistry for insulating fluorine and its compounds.

2. Preparation process

First, let us consider briefly some properties of fluorine. Atomic fluorine is univalent. Only one isotope occurs in nature, stable ^{19}F. As it will be shown in this paper, this property is decisive in the uranium enrichment process. Elemental fluorine is the most reactive and therefore, it forms ionic or covalent fluorides with most of elements even with gold and platinum but except helium, neon, and argon. It has very small dissociation energy (153 kJ/mol) and a very high binding energy: F–C (490 kJ/mol), F–H (570 kJ/mol), or F–S (330 kJ/mol). Under ordinary conditions, fluorine (F_2) is a corrosive pale gas with a yellowish colour. It is a poisonous compound. It causes severe chemical burns in contact with skin. In addition, rapid migration of HF molecule can occur through the skin, reacting with calcium and damaging the bone. Inhalation, except in very low concentrations, is extremely dangerous since it can induce pulmonary oedema.The oxidation state, 1 (0 in F_2) is the only one observed in fluorine compounds. One may note that due to the small size of the fluoride ion (F^-), many stable complexes can be formed with positive ions such as hexafluoroaluminate (AlF_6^{3-}). Fluorine combines with noble gases (krypton, xenon and radon) and reacts vigorously with hydrogen given rise to severe explosions. This last point has therefore a great influence on the electrochemical cell configuration for its industrial preparation as it will be discussed latter. In contact with moist air, fluorine gas reacts with water to form hydrofluoric acid, O_2, F_2O, ...

2.1. Electrochemical cells

Fluorine gas is produced by electrolysis of a fused salt with a composition of KF–*x*HF. Pure HF presents a very low ionic conductivity (10^{-6} S/cm) and then it is necessary to add metal fluoride agent (KF). The phase diagram (Fig. 2) was established by Cady in 1934 [1]. Only two stable phases KF–HF and KF–2HF exhibit low vapour pressure of HF, p_{HF}, around their fused temperature.

2.1.1. "Low temperature" cells

As mentioned above, even if the existence of fluorine was known since the beginning of the XIXth century, nobody succeeded before Henri Moissan in isolating this gas due to its

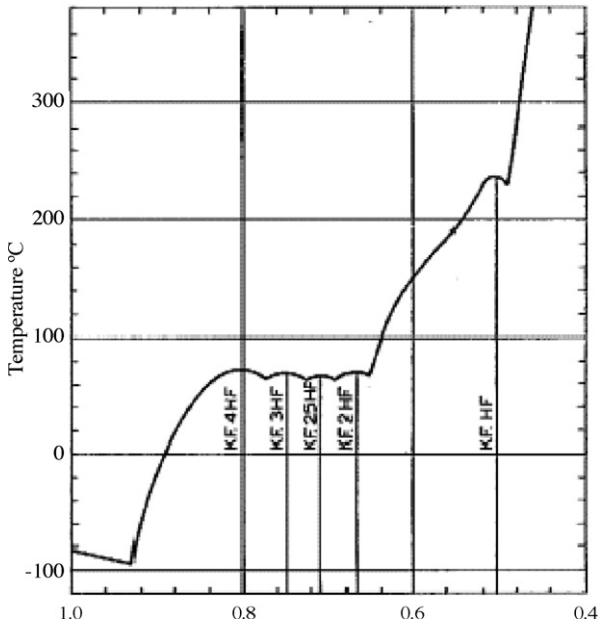

Fig. 2. Phase diagram established by Cady in 1934 [1].

high reactivity. Few years before the discovery of Henri Moissan, Edmond Frémy had almost succeeded in making the electrolysis of fused calcium and potassium using a platinum positive electrode. Frémy observed that this electrode was attacked during the electrolysis due to the reactivity of a gas which cannot be collected. In 1886, and based on the works of Edmond Frémy, Henri Moissan performed the electrolysis of hydrofluoric acid containing a trace of potassium fluoride at temperature below 0 °C. Hydrogen evolved at the negative electrode, whereas an unknown gas was produced at the positive electrode. Henri Moissan made two hypotheses concerning the composition of this gas: fluorine gas or hydrogen perfluoride. After performing the electrolysis of potassium hydrofluoride, he demonstrated that this gas, completely absorbed by hot-red iron (formation of iron fluoride) without any evolution of hydrogen cannot be attributed to hydrogen perfluoride. He isolated for the first time fluorine gas [2–4]. Nevertheless, the "low temperature" cells have never been used on industrial scale for the preparation of fluorine.

2.1.2. "High temperature" cells

The first type of cell built by W.L. Argo in 1919 [5] used a salt of Frémy with a composition of KF–HF at 250 °C. A copper cathode and a graphite anode electrode (unusable in the Moissan's operating conditions) were used. Even if some industrial applications have been reported in Germany during the second world war, this process was rapidly given up because of the temperature of the salt which induces strong difficulties to maintain a constant HF content. Moreover, the fluorine gas is polluted by CF_4 which results from the corrosion of the graphite anode.

2.1.3. "Middle temperature" cells

To solve the problem related to the pollution of fluorine by CF_4, Lebeau and Damiens [6] proposed to perform the electrolysis of KF–3HF at 65 °C < T < 75 °C. The copper container having the salt was used as cathode, the anode was nickel. Cady recommended the use of KF–2.2HF at 75 °C since the vapour pressure of HF in the vicinity of the surface of the melt is lower than that for KF–3HF. Thus, the composition of the electrolyte can be varied in a wide range without generating any significant variation of the temperature.

2.2. Description of the present process

Electrolysis uses the medium temperature cell [7,8]. Indeed, the composition of the fused salt is KF–2HF (40.8 wt% HF) and the temperature is around 95 °C. The optimisation of the process is the result of the efforts of several groups all over the world (Japan, USA, Russia, France, ...). In France, these researches have concerned the study of the electrodes mechanism (at the anode and the cathode) and so, the optimisation of the electrodes materials [9–14], the study of the physico-chemical properties of the electrolyte and its simulation [11,15,16], and of the cell configuration by the computational simulation [17,18].

The problems related to the use of graphite anodes have been solved by using non-graphitised carbon. Indeed, graphite cannot be used as anode materials since exfoliation occurs rapidly during electrolysis. The cell is generally made of steel covered Monel steel cathode electrode is used. In contrast with the chlorine/alkali process in which the distance between the electrodes can be only few millimetres, several centimetres are required to avoid the explosive recombination of anodic (F_2) and cathodic (H_2) gases.

During electrolysis of molten KF–2HF, the fluoride anions involved in the electrochemical reactions are F^- anions solvated by $(HF)_n$ [15,16]. Fluorine and hydrogen are generated according to the two following half-reactions:

$$F(HF)_n^- \rightarrow \tfrac{1}{2}F_2 + nHF + e^-$$

at the anode, and:

$$(n+1)HF + e^- \rightarrow \tfrac{1}{2}H_2 + F(HF)_n^-$$

at the cathode.

The global reaction is written:

$$2HF_{(liq.)} \rightarrow F_{2(g)} + H_{2(g)}$$

This fluorine preparation process [7–22] is characterised by a high current yield of around 0.9 and by a very low energy yield of about 0.3. The latter induces a high production cost compared to other electrolysis processes such as chlorine or aluminium, but are bearable because of the low amount of fluorine gas produced per year (world production of about 15,000 tonnes). Although the thermodynamic decomposition potential of HF is around 2.9 V [21], it is necessary to apply a potential between 8.5 and 10 V to obtain a current density of 12 A dm^{-2}. This voltage is composed of four main contributions: the thermodynamic voltage of HF decomposition, the ohmic drop in the electrolyte, the cathodic overvoltage, and the anodic overvoltage. The high ohmic drop in the electrolyte is due to the large distance between anode and cathode electrodes

as discussed above. The anodic overvoltage is one of the highest among all of the electrolytic processes of inorganic compounds preparation. The understanding of its origin was a great challenge and a lot of fundamental studies were done in past on this subject. Today, the discharge of fluoride ions is better understood.

Let us consider few aspects on the study of the fluorine evolution reaction. These studies have concerned the electrode materials and its surface properties with the properties of the electrolyte and the bubbles shape [22].

2.2.1. Properties of the surface C–F film

It was admitted for a long time that the anodic overvoltage was only due to the formation of a very insulating fluorocarbon C–F film composed of graphite fluorides (denoted CF_x) onto the surface of the carbon anode during electrolysis. The electron transfer through this layer should occur by tunnel effect as in the case of a classical electron transfer through a semiconductor, in other words, the fluorocarbon film acts as an energy barrier which limits the electron transfer during the fluorine evolution reaction. The very low values of the anodic transfer coefficient are effectively in good agreement with such a mechanism involving such a tunnel effect mechanism through a passive film. The fluorocarbon film is intercalated between the electronic conductor (carbon electrode) and the redox couple in solution ($F_2/F(HF)_n^-$). The electrode/electrolyte interface was usually described by the following sandwich structure: $C/CF_x/F_2$/KF–2HF. Nevertheless, the fluorine bubbles generated on a horizontal electrode (Fig. 3) have a lenticular shape and strongly adherent to the surface electrode. The obvious question was therefore: how can one explain that very large current densities ($\geq$1 A/cm^2) are observed taking into account both the presence of an insulating C–F layer and a thick fluorine bubble?

To answer, our attention was focussed not only on the study of the electronic properties and the composition of the C–F film, but also on the influence of the mass transfer at the electrode/electrolyte interface even if this factor should not be taken into account since the electrolysis concerns the main component of the melt.

The properties of the C–F film were studied using various physico-chemical techniques (XRD Raman spectrometry, XPS, STM/AFM, ...) [22]. Among them, atomic probe microscopy provides very useful information. For example, the STM images obtained with a highly oriented pyrolitic graphite (HOPG) sample before and after electro-fluorination in KF–2HF are presented in Fig. 4a and b, respectively [23,24].

Fig. 3. Fluorine bubble generated in KF–2HF on a horizontal electrode facing the top of the electrochemical cell. Reprinted from ref. [43].

This material allows us to reach the atomic resolution. In the case of the raw HOPG sample (Fig. 4a), the typical hexagonal symmetry of HOPG was observed after cleavage: only half of the carbon atoms in a graphene layer generate a high electronic density due to the lamellar structure of graphite. In the case of fluorinated HOPG, three distinct areas were observed:

(i) Insulating areas related to the presence of insulating graphite fluorides (CF_x) with covalent C–F bonds;
(ii) Conductive areas in which the initial hexagonal structure is lost (Fig. 4b) (*i.e.* all the carbon atoms of the hexagonal rings are observed). The spacing between two neighbouring atoms deduced from the corrugation amplitudes is about 0.154 nm. This modification compared to pure HOPG, is due to the intercalation of HF and/or $F(HF)_n^-$ species which increases the distance between two carbon sheets. Moreover, the space located just below the surface is occupied by $F(HF)_n^-$ intercalants, *i.e.* the intercalation of $F(HF)_n^-$ ions forms conducting compound such as fluorine–graphite intercalation compound (F–GIC) with a general formula of $C_x(HF)_yF$.
(iii) Conducting areas where the initial hexagonal structure of HOPG is kept (Fig. 4c), with a periodicity of 0.244 nm. By contrast with pure HOPG, an overlap of the electronic densities between two neighbouring atoms was observed. The fluorination of the surface coupled with the intercalation of $F(HF)_n^-$ anion between two carbon sheets induces the formation of C–F bonds which modify the electronic densities of each carbon atom, *i.e.* another kind of F–GIC (general formula $C_{2n}F$ as shown in Fig. 4d) is formed.

Surface analysis by XPS has shown that the C–F bonds in these two last compounds are ionic and/or semi-ionic type bonding. Additional analyses conducted by AFM coupled with the measurement of the local resistivity on the surface of the same fluorinated HOPG samples [22] have been performed in ambient air with an original laboratory-made device derived from an AFM developed by Houzé [25–27]. It allows covering nine decades of tip/sample resistance value (from 100 Ω to 100 GΩ). The fluorinated HOPG samples previously studied by STM were analysed on 5 μm × 5 μm areas (Fig. 5).

The electrical and topographical images are represented in Fig. 5a and b, respectively; the corresponding distribution of the electrical resistance measured is given in Fig. 5c. As shown in Fig. 5c, the resistance distribution is centred on 3×10^4 and 6×10^{10} Ω average values. For the former, most of the contact resistance values are counted between 8×10^3 and 2×10^5 Ω: this is associated with the red colours on the electrical images (Fig. 5b); for the resistance distribution centred on 8×10^{10} Ω, most of the contact resistance values are counted between 5×10^{10} and 2×10^{11} Ω: this is associated with the purple colours on the electrical images (Fig. 5b). One must notice that the histogram reveals also a continuous variation of the local resistance with two small

shoulders at around 10^7 and 4×10^8 Ω. These images clearly show that the surface of fluorinated HOPG samples does not look uniformly conducting. Note that the presence of less conducting zones does not correspond to transitions between two graphene sheets. As reported in the literature, graphite fluorides and fluorine–graphite intercalation compounds (F–GICs) chemically prepared present a very large difference in term of electrical resistivity. Based on this fact, we interpret the differences of resistivity observed on AFM images with HOPG samples fluorinated in KF–2HF (Fig. 5c) by the presence of F–GICs (with a resistance distribution centred on 3×10^4 Ω), graphite fluorides (with a resistance distribution centred on 6×10^{10} Ω), and intermediate compounds for which the composition varies from CF_x to F–GICs and which give rise to intermediate colours in Fig. 5b from red to purple. To summarise, the C–F film formed during electrolysis of KF–2HF presents a high heterogeneity of composition due to the presence of conducting F–GICs and insulating CF_x.

2.2.2. Schematic representation of the electrode/electrolyte interface

Our interest was focussed also on the study of the influence of the mass transfer at the electrode/electrolyte interface by electrochemistry.

A typical chronoamperogram obtained in KF–2KF is presented in Fig. 6: a galvanostatic pulse was applied to the electrode at $t = 0$. The current density, j, reaches rapidly a maximum value. Then, a slow decrease of j is observed. The lateral coalescence of the fluorine bubbles continues until a complete coverage of the surface electrode. When the bubble volume is maximum, the gas bubble evolves and again the current density reaches a maximum value lower than the one obtained at the beginning of the pulse. One important observation is that the current density never reaches a null value as expected. These analyses, completed by other electrochemical tests of experiments notably by impedancemetry and cyclic voltammetry allow us to propose a new schematic representation of the carbon/KF–2HF interface [23]

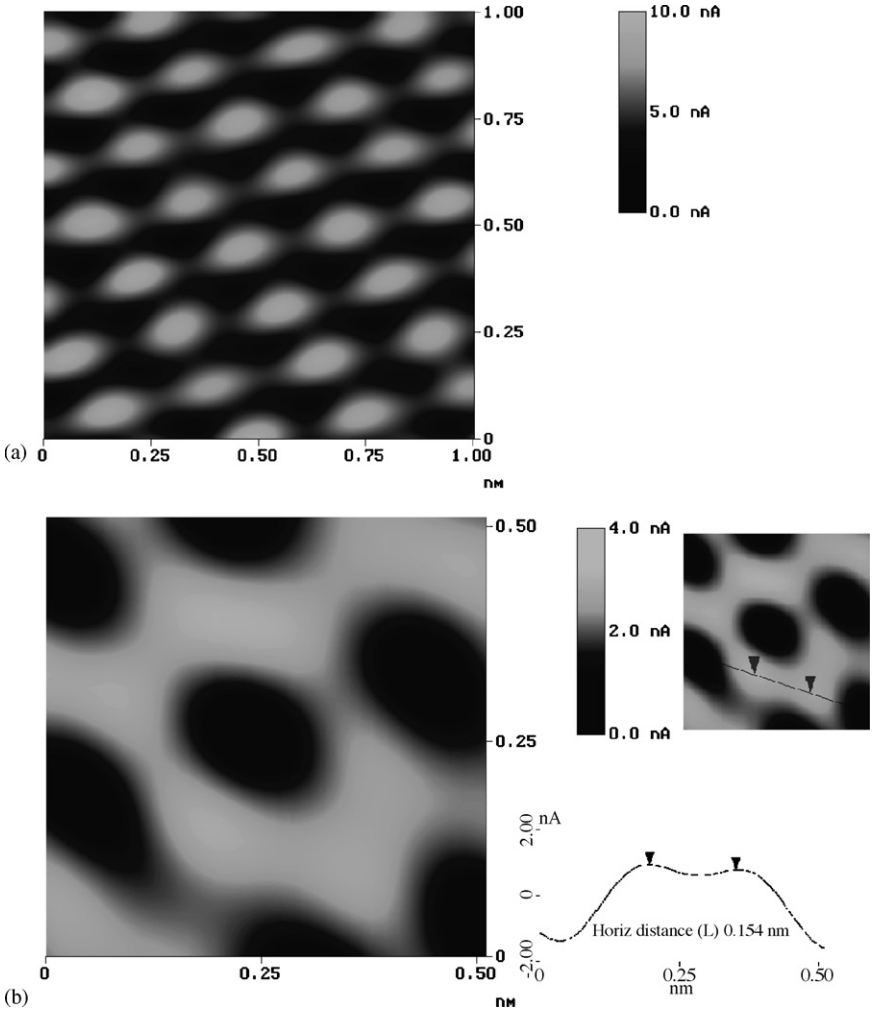

Fig. 4. (a) STM image of pure HOPG. Experimental conditions: bias voltage: 20 mV; setpoint: 4 nA; z range: 5 nA; constant height mode; Pt/Ir tip. (b) STM image and cross-section of HOPG passivated at 6 V in KF–2HF ($C_{H_2O} < 20$ ppm) during 30 min. Experimental conditions: bias voltage: 20 mV; setpoint: 4 nA; z range: 5 nA; constant height mode; Pt/Ir tip. (c) STM image and cross-section for HOPG passivated at 6 V in KF–2HF ($C_{H_2O} < 20$ ppm) during 30 min. Experimental conditions: bias voltage: 20 mV; setpoint: 4 nA; z range: 3 nA; constant height mode; Pt/Ir tip. Reprinted from ref. [44]. (d) Schematic in-plane structural model for fluorinated HOPG. The centred hexagonal lattice commensurate with the graphite lattice is shown. Open circles: bonded C atoms (reprinted from ref. [24]).

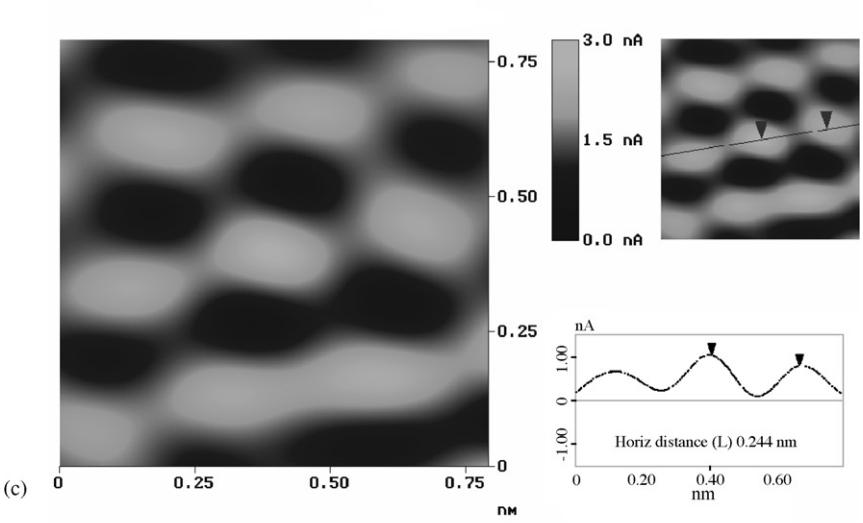

(c)

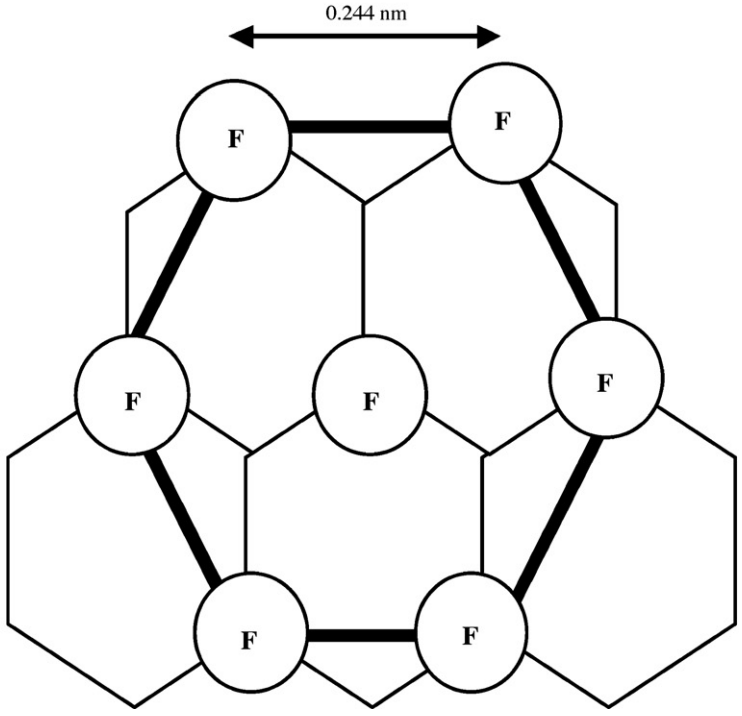

(d)

Fig. 4. (*Continued*).

involving a heterogeneous and conducting layer (called ''dispersed'' layer) in which the liquid electrolyte (KF–2HF) and dissolved fluorine until saturation co-exist. This layer, in which the current flows, is intercalated between the C–F layer and the gas bubble, the latter growing by diffusion of fluorine through the dispersed layer. This new representation is given in Fig. 7.

The new schematic representation of the carbon/KF–2HF interface presented in Fig. 7 allows us to have a better understanding on the origin of the total anodic overvoltage, η_T, which characterises the FER: it is not only due to the C–F film present on carbon anodes but also to the ''dispersed'' layer, *i.e.* η_T is equal to the sum of two terms: η_{C-F} (activation overvoltage for the fluorine evolution reaction) and $\eta_{disp.}$ (ohmic drop in the ''dispersed'' layer). In the case of horizontal electrode facing the top of the electrochemical cell, numerical calculations were performed to determine each contribution *versus* the electrode radius, r_0, and the resistivity, ρ, of the ''dispersed'' layer [22,23]. To succeed, a model was developed and the reaction mechanism is analysed by numerical simulation in order to determine the exact contribution of η_{fluid} and η_{C-F} to η_T. These results have confirmed that the presence of the ''dispersed'' layer cannot be neglected for a good understanding of the fluorine evolution process. For instance, it was found that $\eta_{disp.}$ and η_{C-F} (Fig. 8) were equal to 1 and 1.5 V, respectively, for $\rho = 10\ \Omega$ cm (resistivity of the ''dispersed'' layer), $T = 95\ ^\circ$C and $r_0 = 0.8$ cm.

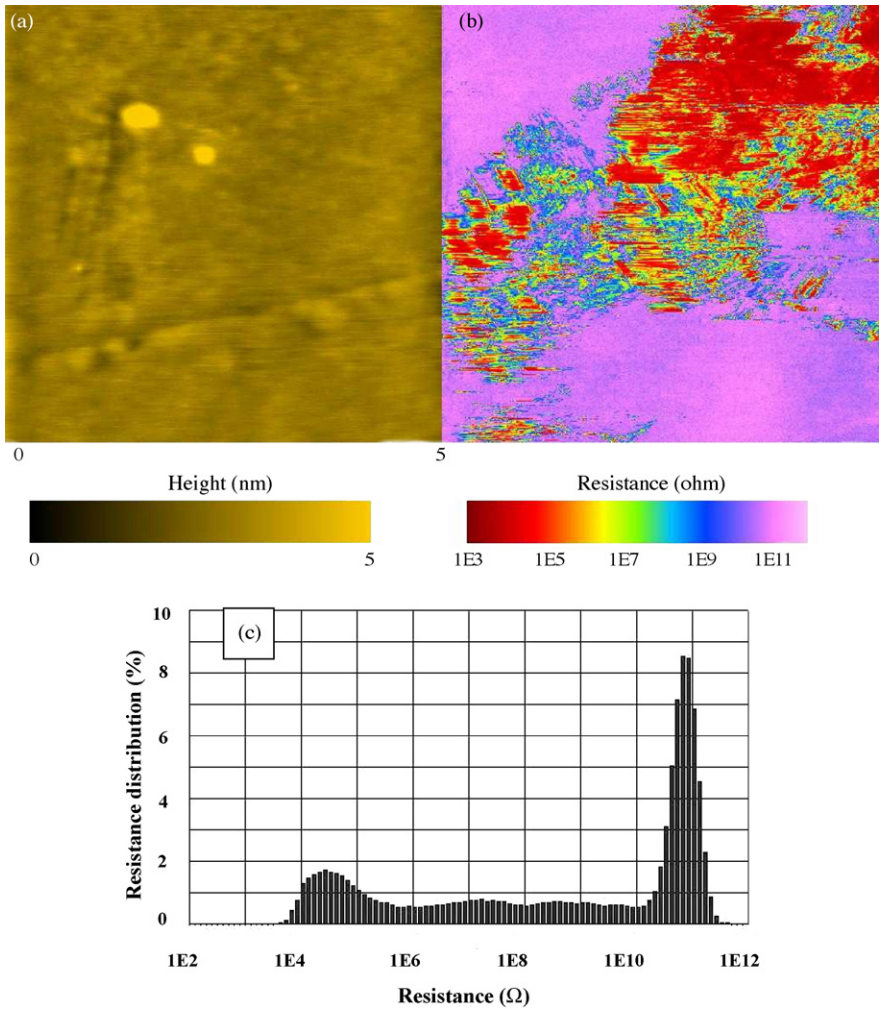

Fig. 5. AFM investigations on HOPG fluorinated in KF–2HF at 6 V: (a) topographical image; (b) electrical image; (c) distribution of the measured resistance deduced from (b). Reprinted from ref. [22].

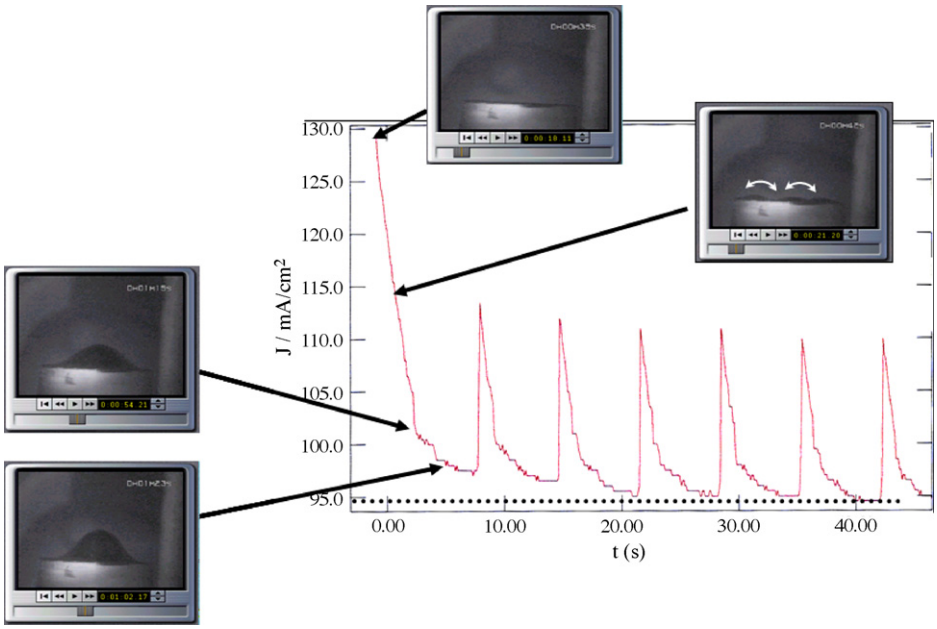

Fig. 6. Typical chronoamperogram obtained on carbon anode in KF–2HF. Applied potential: $E = 4.5$ V *vs.* Cu/CuF_2.

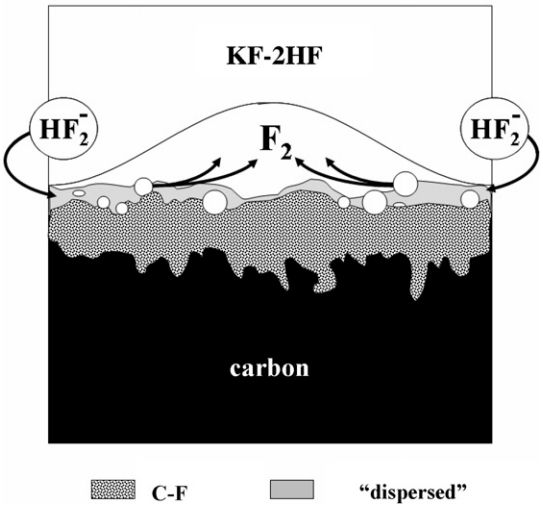

Fig. 7. Schematic representation of the electrode/electrolyte interface. Reprinted from ref. [43].

2.2.3. Study of fluorine bubble shape

The model which described from a fundamental point of view the intimate process of the fluorine evolution process and the influence of surface tension at the electrode/electrolyte interface (described in detail in refs. [22,23]) was slightly improved taking into account the importance of the capillary forces, the surface tension and the internal pressure in the bubble [28]. Indeed, the bubble shape is not predicted by the classical theory which assumes that the interface profile depends only on a constant gas–liquid interfacial tension. It results in that the bubble surface should exhibit a constant curvature radius, in contrast to the experimental observations. Such a distortion reflects certainly the strong attraction of the fluorine by the electrode surface. To describe the phenomenon, it was assumed that a long-range force F acts on the gas molecules [29]. Moreover, in order to calculate the shape of the gas bubble, it was necessary to consider the different forces acting at the interface. These forces give rise to five different pressure terms; the pressure, p_{bub}, of the gas inside the bubble, the atmospheric pressure, p_{atm}, the hydrostatic pressure, p_{hyd}, the pressure, p_{int}, due to the interfacial tension at the gas–liquid interface and the pressure, p_{att}, due to the gas–electrode attraction [30].

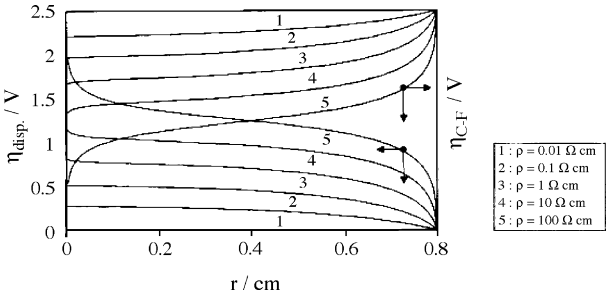

Fig. 8. Variation of (a) the overvoltage in the "dispersed" layer, $\eta_{disp.}$, in the C–F layer, η_{C-F}, for several values of the resistivity ρ of the "dispersed" layer. $\eta_T = 2.5$ V, $T = 95$ °C. Reprinted from ref. [43].

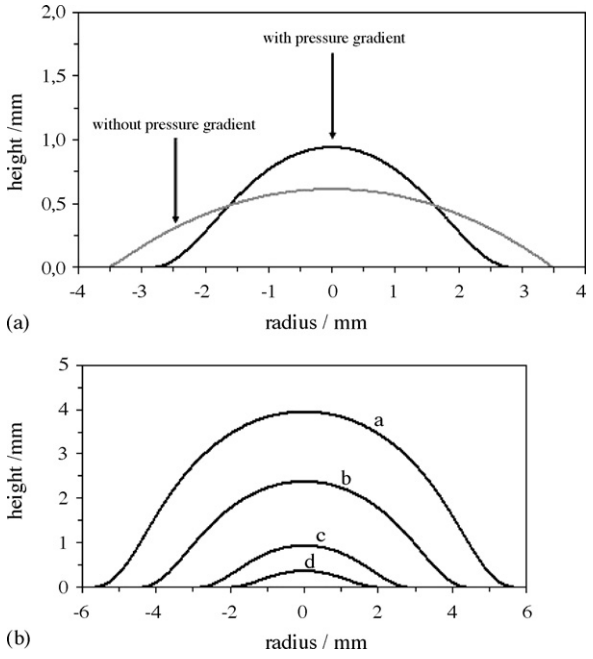

Fig. 9. (a) Profiles of a bubble containing 3.7×10^{-7} mol of fluorine gas calculated from the classical theory and from the present theory introducing a pressure gradient. (b) Grow of gas bubbles according to the present theory introducing a pressure gradient. Number of gas moles in the bubbles (a) 6.0×10^{-8}; (b) 3.7×10^{-7}; (c) 2.7×10^{-6}; (d) 8.4×10^{-6}. Reprinted from ref. [30].

To illustrate the influence of the pressure gradient, the bubble profiles of the two gas bubbles, a and b, containing the same amount of gas (3.7×10^{-7} mol) are presented in Fig. 9a. The bubble without a pressure gradient is deduced from the classical theory (constant interfacial pressure) for a wetting angle $\theta = 10°$. The second profile takes into account the pressure gradient, the wetting angle is $\theta = 0°$. Two main differences appear. An important flattening of the borders is seen in the bubble with a pressure gradient. The volume of the spherical cap is much larger than the volume of the bubble with a pressure gradient. This is due to the fact that, for an external pressure of 1 atmosphere (atm), the internal pressure in bubble without a pressure gradient is 1.0034 atm and the mean pressure in bubble with a pressure gradient is 1.375 atm [30].

The effect of the gas attraction by the electrode surface induces also a considerable modification in the bubble growth. Thus, the calculated profiles for bubbles containing different quantities of gas are presented in Fig. 9b [30]. The introduction of a variable pressure tends to elongate the bubble shape toward the top of the cell as expected. This elongation is not observed if the variable pressure is not taken into account. The calculated shapes of the bubbles given in Fig. 9b are in good agreement with *in situ* observations (Figs. 3 and 4).

2.2.4. Improvements of the fluorine preparation process

Finally, one must mention efforts done by several groups notably in Japan, USA and France to improve the fluorine evolution process mainly by the modification of the local composition of the C–F film. This is performed by inserting a metallic agent such as Al, Mg, ... [31–38]. The improvements

of the fluorine evolution reaction were due to formation of fluorine–graphite intercalation compounds containing small traces of metal fluorides. The formation of such compounds reduces the influence of the CF_x groups on the total wettability of the electrode by KF–2HF and so, improves the fluorine bubbles detachment. Another way approach was proposed by Childs and Bauer [39] who proposed a new design of the carbon anodes containing vertical channels. The aim was to enhance the movement of fluorine bubbles up the face of the anode to the electrolyte surface. With such a design, the authors reported the possibility to operate in KF–2HF at high current density for a very long time without polarising. Moreover, the current efficiency was found to be near 100%. Recently, Tojo et al. proposed, for a new concept of small type of fluorine cell with high capacity, the use of boron-doped diamond (BBD) covered carbon electrodes prepared by hot-filament chemical vapour deposition [40]. They showed that such electrodes enable the electrolysis of KF–2HF at a high current density (up to 100 A dm^{-2}) without the occurrence of anode effect.

The researches done all over the world during many years to improve our knowledge on the fluorine evolution mechanism can be easily explained by the key role of fluorine gas in the nuclear process, as it will be shown hereafter.

3. Fluorine gas in the nuclear field

3.1. The present situation

After the oil crisis in the 1970s, many countries have decided to strongly develop nuclear energy, notably in France. In the latter, 58 nuclear plants are still running and the part of nuclear for the production of electricity is about 80%. Twenty-two reactors are under construction in the world notably eight in China, four in Ukraine, three in Japan, and in Finland the first nuclear plant of the 3rd generation (*European Pressurised Reactor*, *denoted EPR*) in the world is under construction. The nuclear energy represents about 17% of the world production of electricity, about 35% in the European Community. In France, Electricity of France (EDF) has decided to construct a new plant using the EPR technology in Flamanville (Manche).

The predictions in term of energy show that the energy consumption in the world should be about twice up to 2020 not only due to the increase of the energy demand in the industrialised countries but also to the increase of the population and the industrialisation of the emergent countries notably in Asia and in Latin America. Therefore, the contribution of nuclear energy should increase since the fossil resources should decrease and because the potential of renewable energy is too low for the moment, even if the latter should increase in a near future.

3.2. Preparation of the fuel [41,42]

Uranium is a grey-white metal with a higher density than lead. It is present chemically combined in almost all media (rocks, water, ...) even if in very small proportion. The present deposits contain usually several hundreds of grams to several kilograms of uranium per ton of extracted minerals. However, some of them with exceptional content of U are under exploitation in Canada with uranium content higher than few tens of kilograms of extracted minerals. The main deposits are located in Africa (Niger, South Africa, Namibia), Australia, Canada, Kazakhstan, Uzbekistan and Russia.

Whatever the uranium content in the minerals used for its extraction, U is present mainly in two isotopic forms: 99.28% of ^{238}U (fertile) and 0.71% of ^{235}U (fissile). Only ^{235}U can release from energy by fission in the majority of nuclear plants. The latter use uranium which contains between 3 and 5% of ^{235}U. Therefore, an uranium enrichment process is done from UF_6 (only volatile compound of uranium) not only because its relative chemical stability and its low sublimation temperature, but also because fluorine has only a single stable naturally occurring isotope (^{19}F) as reported above. Therefore, isotopomeres of UF_6 differ in their molecular weight only because of U.

The industrial process to obtain UF_6 from the ores takes place according the following mechanism:

$$U_3O_8 \xrightarrow{HNO_3} UO_2(NO_3)_2 \xrightarrow{\Delta T} UO_3 \xrightarrow{H_2} UO_2 \xrightarrow{HF} UF_4 \xrightarrow{F_2} UF_6$$

In the two last steps, UO_2 is converted with hydrofluoric acid (HF) to UF_4 and then the oxidation with fluorine gas finally yields UF_6. The conversion of UF_4 to UF_6 is performed in a flame reactor and is a very exothermic process: temperature of about 1100 °C can be reached in reactors.

Let us consider some properties of UF_6. It is a colourless gas above 64 °C and a white solid at room temperature. The liquid phase only exists under pressures greater than about 1.5 atmospheres and at temperatures above 64 °C. UF_6 is an oxidant and a Lewis acid. It reacts with many elements such as Al, Ga, C, ... to form their fluorides and attacks many metals except Ni and Al on which a passivating and protective metal fluoride layer is formed. It does not react with oxygen, nitrogen, carbon dioxide and halogens (in vapour phase). However, it is very hygroscopic and reacts with water to give uranyl fluoride (UO_2F_2) and HF. Presence of metallic impurities induces a yellowish colour.

The two main industrial enrichment processes are the gaseous diffusion and the gas centrifugal method. Note that the first one requires much higher energy than the gas centrifugal process. For these two processes, UF_6 is used because of its triple point at 64 °C.

The gaseous diffusion process is based on the small mass difference between the two uranium isotopes. UF_6 gas is forced to diffuse under pressure through micropores with a radius lower than the main free path of the molecules. The lighter molecules ($^{235}UF_6$) diffuse slightly faster than the $^{238}UF_6$ molecules. Therefore, the enriched fraction is injected to the upper level and the depleted fraction comes back to the lower level. This process is repeated more than one thousand times to reach UF_6 containing between 3 and 5% of ^{235}U.

The gas centrifugal process is based on the same phenomenon considering the mass difference between the two isotopes. UF_6 is introduced into centrifugal rotating at high speed. The lighter molecules are concentrated at the centre of the centrifugal. A vertical separation is established with a

gradient from the lighter at the top to the heaviest at the bottom. The enriched fraction is collected from the head of the centrifugal and the depleted one at the bottom. Several thousands of centrifugals are necessary to obtain industrial capacities compatible with the requirements of an electro-nuclear park. In a near future, this technology will be used instead of gaseous diffusion since the latter consumes too much energy (required power of 2500 MWe).

The enriched UF_6 is then converted by chemical reduction to uranium oxide (UO_2) packaged as small pellets of a ten of grams which are sintered at high temperature. Then, the pellets are introduced in long metallic tubes composed of zirconium alloys hermetically closed. These are finally introduced in the hole of the reactor. Their average residence time is comprised between 4 and 5 years before being changed.

As already mentioned in this paper, the production of electricity from nuclear plants should grow up in the next decade to satisfy the energetic demand all over the world. In spite of the advantages offered by nuclear in term of low cost of kWh and energetic independence, the main encountered problem is the treatment, the maintenance and the storage of radioactive wastes. Industrial recycling of radioactive materials contained in the nuclear fuels is done in only few countries (France, Russia, and United Kingdom). Ninety-six percent of the used fuel (in mass) is recovered. Uranium with the same content in fissile uranium close to natural uranium will be used again as described previously. Recycling of uranium allows saving about 15% of the requirements of natural uranium. The extracted plutonium (1%) allows producing a new fuel called ''MOX'' (*i.e.* mixed oxides) composed of a mixture of uranium and plutonium oxides. This fuel is already used in a third of 900 MW French water pressure reactors: the fission of one gram of Pu allows producing the same quantity of electricity than 2 tonnes of oil. The ultimate wastes (3% of non-recycling fuel and highly radioactive) are incorporated and immobilised into a glass lattice. They cool during about 30–40 years before their transfer in sites for final storage.

However, one must remind that the production of electricity *via* nuclear plants does not contribute to the emission of pollutants such sulphur dioxide (SO_2), nitrogen oxide (NO_x) and carbon dioxide (CO_2) contributing notably to the greenhouse effect. Thus, such energy production mode avoids the emission of several hundreds of tonnes of CO_2 per year in France.

Taking into account the world energy context, and if one considers that the production of UF_6 and the enrichment of uranium do not change in the next decades, the UF_6 requirement (and consequently that of F_2) should increase drastically. In addition, the fluorine demand with high purity is also very important notably in the field of microelectronic. Therefore, improvements of the present fluorine production process, notably the reduction of the anodic overvoltage, can be considered as essential to satisfy the future requests.

Acknowledgements

This paper is mainly extracted from another one published in the French journal ''L'Actualité Chimique'' (October–November 2006, number 301–302). The authors would like to acknowledge Pr. Didier Devilliers (Laboratoire LI2C CNRS UMR 7612, Paris, France) for helpful and fruitful discussions, Michel Combel and Alain Colisson (Laboratoire R&D de AREVA/Comurhex Pierrelatte, France) for their helpful assistance in the electrochemical tests, Dr. Serge Durand-Vidal (Laboratoire LI2C-CNRS UMR 7612, Paris, France) for making the STM investigations, Dr. Frédéric Houzé (Laboratoire de Génie Electrique de Paris-UMR CNRS 8507, France) for the measurements of the local resistivity by AFM, and Dr. Jean-Pierre Caire (ENSEEG, Saint Martin d'Hères, France) for fruitful discussions.

References

[1] G.H. Cady, J. Am. Chem. Soc. 56 (7) (1934) 1431–1434.
[2] H. Moissan, C.R. Acad. Sci. 102 (1886) 1543–1544.
[3] H. Moissan, C.R. Acad. Sci. 103 (1886) 202–205.
[4] H. Moissan, C.R. Acad. Sci. 103 (1886) 256–258.
[5] W.L. Argo, F.C. Mathers, B. Humiston, C.O. Anderson, J. Phys. Chem. 23 (1919) 348–355.
[6] P. Lebeau, A. Damiens, C.R. Acad. Sci. 181 (1925) 917–919.
[7] M. Jaccaud, F. Nicolas, Techniques de l'Ingénieur (1990) J1453–J6020.
[8] D. Devilliers, O. Tillement, M. Vogler, l'Actualité Chimique 1 (1992) 5–34.
[9] D. Devilliers, Thesis, P. & M. Curie University, Paris, 1984.
[10] S. Lamirault, Thesis, P. & M. Curie University, Paris, 1987.
[11] S. Rouquette, Thesis, P. & M. Curie University, Paris, 1989.
[12] B. Teisseyre, Thesis, P. & M. Curie University, Paris, 1988.
[13] H. Groult, HDR Thesis, P. & M. Curie University, Paris, 2003.
[14] S. Rouquette-Sanchez, D. Ferry, J. Picard, Electrochem. Soc. 136 (1989) 3299–3308.
[15] C. Simon, Thesis, P. & M. Curie University, Paris, 2001.
[16] C. Simon, T. Cartailler, P. Turq, J. Chem. Phys. 117 (2002) 3772–3779.
[17] H. Roustan, Thesis, National Polytechnic Institute of Grenoble (INPG), Grenoble, 1998.
[18] H. Roustan, J.-P. Caire, F. Nicolas, P. Pham, J. Appl. Electrochem. 28 (1998) 237–243.
[19] A.J. Rudge, in: A.T. Khun (Ed.), Industrial Electrochemical Processes, Elsevier, Amsterdam, 1971 (Chapter 1).
[20] D. Pletcher, Industrial Electrochemistry, Chapman and Hall, London, 1982 (Chapter 5).
[21] D. Devilliers, F. Lantelme, M. Chemla, J. Chim. Phys. 76 (1979) 428–432.
[22] H. Groult, C. Simon, A. Mantoux, F. Lantelme, P. Turq, in: T. Nakajima, H. Groult (Eds.), Fluorinated Materials for Energy Conversion, Elsevier, 2005, pp. 1–29 (Chapter 1).
[23] H. Groult, F. Lantelme, J. Electrochem. Soc. 148 (2001) E13–E18.
[24] H. Groult, D. Devilliers, S. Durand-Vidal, F. Nicolas, M. Combel, Electrochim. Acta 44 (1999) 2793–2803.
[25] F. Houzé, R. Meyer, O. Schneegans, L. Boyer, Appl. Phys. Lett. 69 (1996) 1975–1977.
[26] J.P. Kleider, C. Longeaud, R. Brüggemann, F. Houzé, Thin Solid Films 383 (2001) 57–60.
[27] S. Guessab, L. Boyer, F. Houzé, S. Noël, O. Schneegans, Synth. Met. 118 (2001) 121–132.
[28] F. Lantelme, H. Groult, J. Electrochem. Soc. 151 (2004) D121–D126.
[29] P.-G. de Gennes, F. Brochard-Wyart, D. Quéré, Gouttes, Bulles Perles et Ondes, Berlin, Paris, 2002, p. 83.
[30] F. Lantelme, H. Groult, C. Belhomme, B. Morel, F. Nicolas, J. Fluorine Chem. 127 (2006) 704–707.
[31] T. Nakajima, T. Ogawa, N. Watanabe, J. Electrochem. Soc. 134 (1987) 8–11.
[32] D. Devilliers, B. Teysseyre, M. Chemla, Electrochim. Acta 35 (1990) 153–162.
[33] P.T. Hough, D.M. Novak-Antoniou, US Patent 4,602,985 (1986).

[34] N. Watanabe, M. Inoue, S. Yoshizawa, J. Electrochem. Soc. Japan 31 (1963) 113–117.
[35] T. Tojo, Y.-B. Chong, N. Watanabe, in: Proceedings of 12th International Symposium on Fluorine Chemistry, Santa-Cruz, USA, 1988 (abstract no. 408).
[36] T. Tojo, J. Hiraiwa, M. Dohi, Y.-B. Chong, N. Watanabe, J. Fluorine Chem. 54 (1991) 136.
[37] Asahi Glass Co., J.P. Kokai, Patent 58,81,981 (1983).
[38] O.R. Brown, M.J. Wilmott, European Patent 255,225 (1988).
[39] W.V. Childs, G.L. Bauer, J. Electrochem. Soc. 142 (1995) 2286–2290.
[40] T. Tojo, H. Takebayashi, N. Watanabe, 18th International Symposium on Fluorine Chemistry, Bremen (Germany), 2006 (abstracts APPL_001).
[41] http://www.arevagroup.com.
[42] P. Blanpain, G. Capus, J.-C. Palussière, Chimia 59 (2005) 894–897.
[43] H. Groult, J. Fluorine Chem. 119 (2003) 173–189.
[44] H. Groult, S. Durand-Vidal, D. Devilliers, F. Lantelme, J. Fluorine Chem. 107 (2001) 247–254.